

Chemistry–A European Journal

Supporting Information

Localized Crystallization of Calcium Phosphates by Light-Induced Processes

Patricia Besirske, Arianna Menichetti, Marco Montalti,* Juan Manuel García-Ruiz,*
Martin Winterhalder, Johannes Boneberg, and Helmut Cölfen*

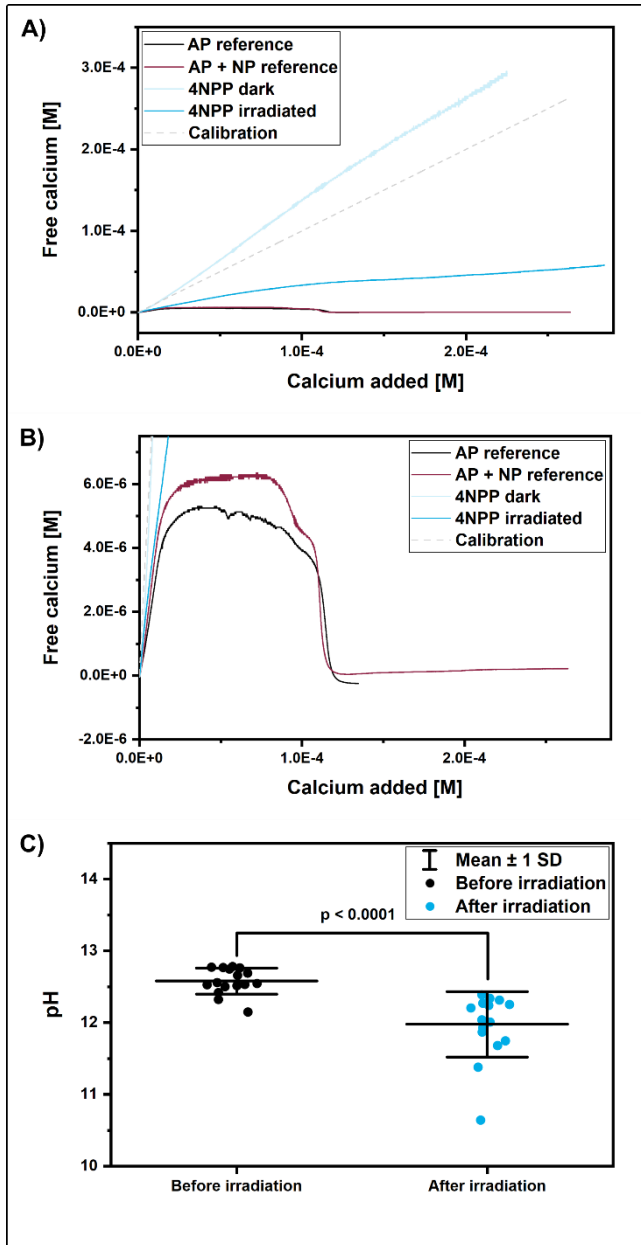


Figure 1. A) Titration curve of the ammonium phosphate reference substance (black), the irradiated (dark blue) and non-irradiated (light blue) 4NPP as well as the ammonium phosphate with an additional share of byproduct (dark red). B) Cutout of Figure A). C) pH trend before and after irradiation. Origin 2020 paired sample t test with $p = 6.3680 \cdot 10^{-5}$ (SD = standard deviation).

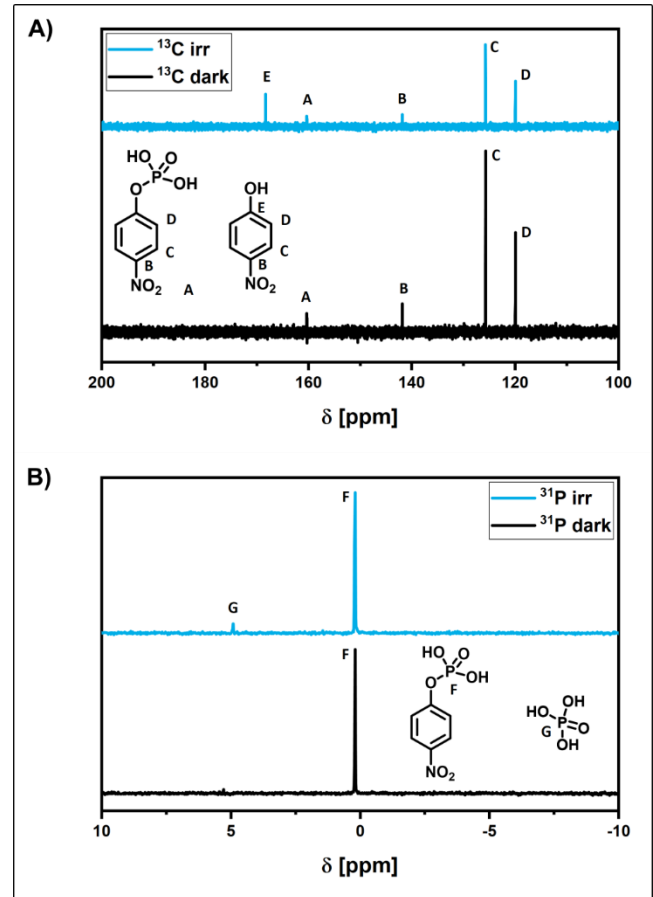


Figure 2. A) ^{13}C NMR of the irradiated (blue) and non-irradiated (black) 4NPP solution. B) ^{31}P NMR of the irradiated (blue) and non-irradiated (black) 4NPP solution.

Dark:

^{13}C -NMR: (600 MHz, D_2O): δ (ppm) = 160.34 (arom. $\underline{\text{C}}\text{-O-P}$); 141.82 (p -arom. $\underline{\text{C}}\text{-NO}_2$); 125.73 (m -arom. $\underline{\text{C}}\text{H}$); 119.97 (o -arom. $\underline{\text{C}}\text{H}$).

^{31}P -NMR: (800 MHz, D_2O): δ (ppm): = 0.20 (arom. $\underline{\text{C}}\text{-O-P}$).

Irradiated:

^{13}C -NMR: (600 MHz, D_2O): δ (ppm) = 168.28 (arom. $\underline{\text{C}}\text{-OH}$); 160.35 (arom. $\underline{\text{C}}\text{-O-P}$); 141.83 (p -arom. $\underline{\text{C}}\text{-NO}_2$); 125.74 (m -arom. $\underline{\text{C}}\text{H}$); 119.98 (o -arom. $\underline{\text{C}}\text{H}$).

^{31}P -NMR: (800 MHz, D_2O): δ (ppm): = 4.92 ($\underline{\text{P}}\text{O}_4^{3-}$); 0.20 (arom. $\underline{\text{C}}\text{-O-P}$).

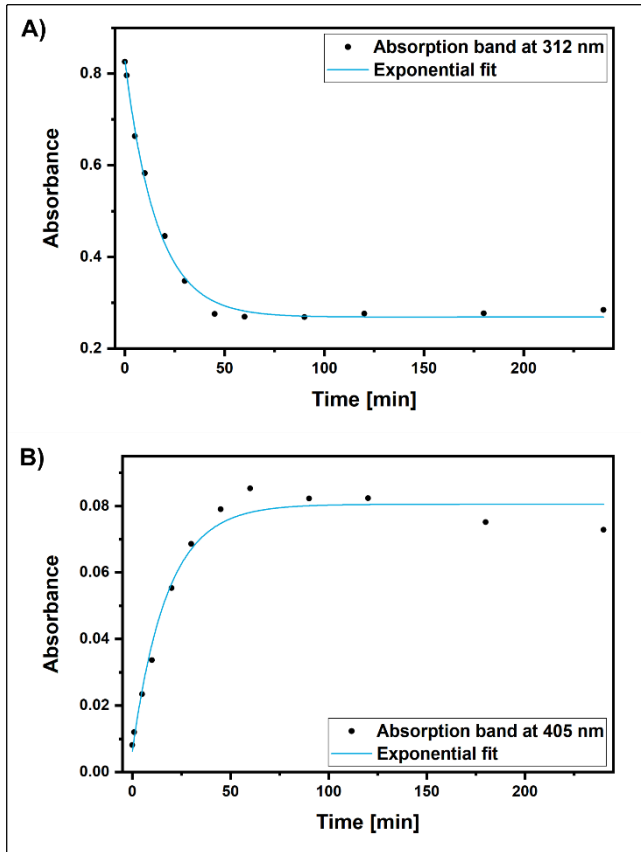


Figure 3. A) Exponential decay of the absorption band at 312 nm referring to the starting material 4NPP. B) Limited growth of the absorption band at 405 nm referring to the byproduct 4-Nitrophenolate (4NP).

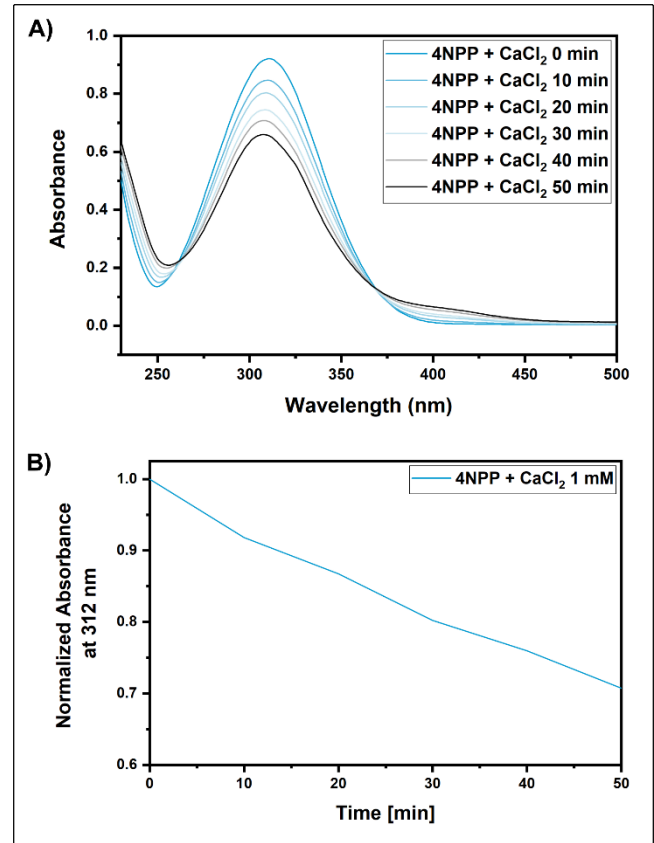


Figure 4. A) Measurement data of the UV/Vis measurement of 4NPP irradiated with UV light over time for determination of the photoreaction quantum yield. B) Normalized absorbance at 312 nm of a CaCl₂ containing 1 mM 4NPP solution.

$$\phi \sim ([R_0] - [R_t]) \cdot \frac{V \cdot N_A}{q_{p,in} \cdot t}$$

$[R_0]$ = 4NPP molar concentration at $t = 0$ min (1 mM);

$[R_t]$ = 4NPP molar concentration at time $t = 50$ min (0.7 mM, calculated by the absorbance value at 312 nm);

$V = 0.0025$ L;

$N_A = 6.02 \times 10^{23} \text{ mol}^{-1}$ (Avogadro number);

$q_{p,in} = 0.95 \times 10^{16} \frac{\text{number of photons}}{\text{s}}$ (incident photon flux);

t = irradiation time [s]

ϕ = quantum yield

$A_{0 \text{ min}}$ and $A_{50 \text{ min}}$ are absorbances of 4NPP 1 mM at 365 nm at the beginning (0 min) and the end (50 min) of the irradiation.^[1]

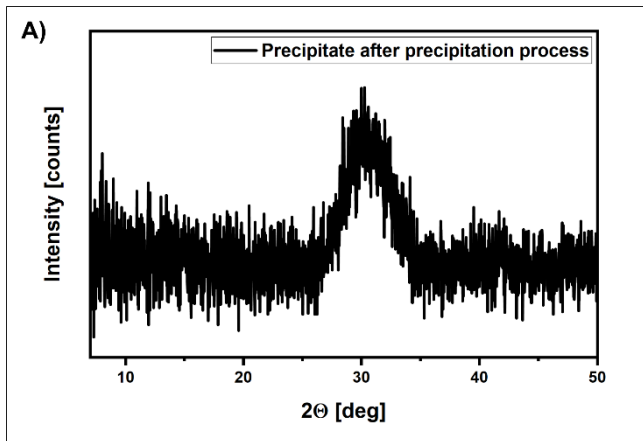


Figure 5. pXRD measurement of the unheated precipitate directly after the precipitation process. No sharp reflexes are detectable indicating that the precipitate formed is amorphous.

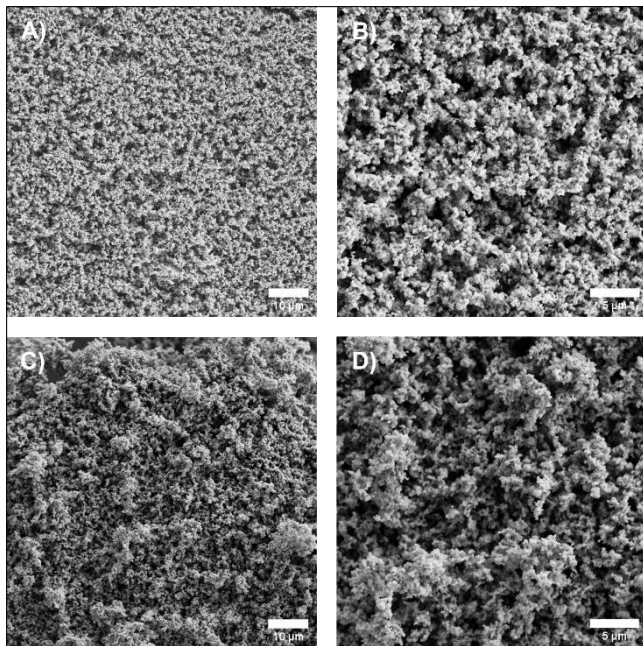


Figure 6. A) and B) Precipitate directly after the precipitation process. C) and D) Precipitate after the heating treatment.

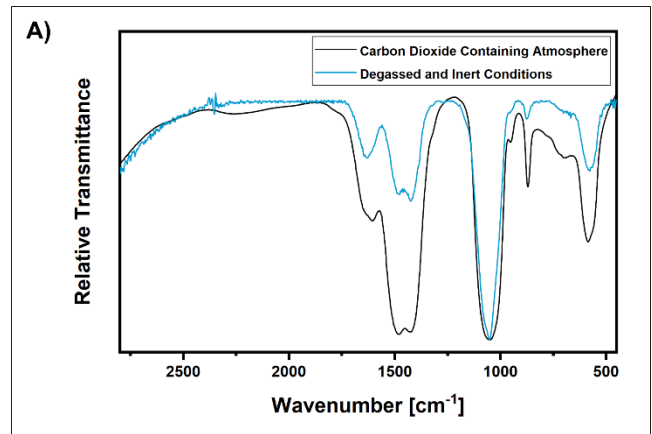


Figure 7. Influence of the carbon dioxide content present during the precipitation process influencing the carbonate content in the final precipitate.

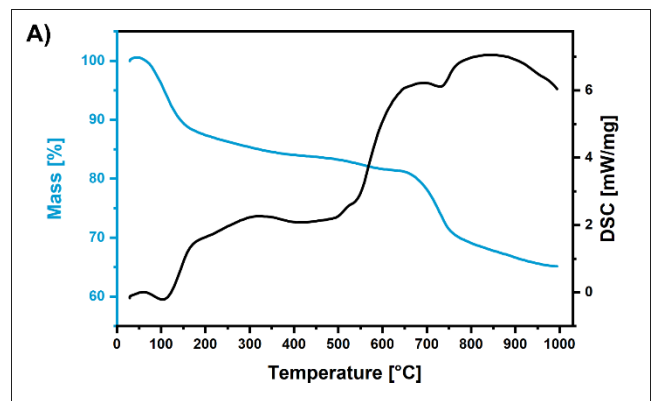


Figure 8. A) TGA measurement of the precipitate. The blue curve represents the mass loss during the decomposition process, whereas the black curve depicts the differential scanning calorimetry (DSC) measurement.

The thermal decomposition of the material is depicted in **Figure 8** in the blue curve. The decomposition is subdivided into two big steps. In the first stage, from 30 to 160 °C, 12 % weight loss was observed. This weight loss can be attributed to the loss of adsorbed water. Between 300 and 600 °C carbonate evolution takes place.^[2] This could be due to a structural relocation of carbonate as a consequence of a reaction between hydrogen phosphates and carbonates and therefore lead to the slow decrease of the mass. The second sharp decrease of 16 % from 650 °C on, is attributed to the decarbonation of the material. The differential scanning calorimetry (DSC) measurement is represented by the black curve. Around 100 °C the evaporation of water is visible as in the TGA measurement. Two exothermic peaks were identified at 420 °C and 730 °C. The first one could be due to the crystallization of the material. The second one corresponds to the decarbonation and rearrangement of the carbonate and phosphate groups present in the carbonate hydroxyapatite. All in all, the DSC measurement is in good agreement with the thermogravimetric analysis.^[3]

Table 1. Correlation of the chemical shift with the carbon and phosphor atoms of the substances.

Signal	Correlation	Chemical shift [ppm]	Literature
A	arom. \underline{C} -O-P	160.34	[4]
B	<i>p</i> -arom. \underline{C} -NO ₂	141.82	[4]
C	<i>m</i> -arom. \underline{C} H	125.73	[4]
D	<i>o</i> -arom. \underline{C} H	119.97	[4]
E	arom. \underline{C} -OH	168.28	[5]
F	arom. C-O- \underline{P}	0.20	[6]
G	\underline{P} O ₄ ³⁻	4.92	[6]

Table 2. Correlation of the measured IR-vibration bands with known IR-bands in literature.

Wavenumber [cm ⁻¹]	#	Vibration	Literature
3384	A	O-H stretching vibration of free water molecules	[7]
2246	B	R ₂ P(O)OH	[8]
1627	C	Double band H-O-H binding vibration, water of crystallization	[9]
1488	D	C-O stretching vibration	[9-10]
1424	E	C-O stretching vibration	[9-10]
1049	F	P-O stretching vibration	[7, 9, 11]
952	G	Totally symmetric P-O stretching vibration	[9, 11]
871	H	C-O binding vibration	[9-10]
697	I	C-O stretching vibration	[9, 12]
580	J	Antisymmetric P-O binding vibration	[7, 9, 11]

Experimental Section

Devices

Magnetic Resonance (NMR) spectroscopy characterizations (¹H, ¹³C, ³¹P) were carried out using a JEOL JNM-ECZ500R/S1 (500 MHz) as well as a Bruker Avance III 600 (600 MHz) and a Bruker Avance III 400 (400 MHz). These experiments were operated at room temperature. For cryogenic ³¹P experiments a Bruker AVANCE NEO 800 (800 MHz) was used.

Fourier-Transform Infrared Spectroscopy (FTIR)-spectra were prepared using a Perkin Elmer 100 Spectrum spectrometer with a Universal Attenuated Total Reflection (UATR) sampling accessory. Therefore, a share of the sample was mortared with potassium bromide and pressed into a pellet with a force of 5 tonnes for half an hour.

Raman measurements were performed with a MonoVista CRS system by S&I Spectroscopy & Imaging GmbH. The used microscope is a custom-made product by Leica Microsystems GmbH which includes a Leica TCS SP8 CARS / SRS with a picoEmerald laser system by APE Angewandte Physik & Elektronik GmbH.

UV/Vis absorption spectra were performed in a Varian Cary 50 UV-Vis Spectrophotometer in a quartz cuvette. The spectra were measured from 200 to 800 nm and from 250 to 500 nm in the case of the kinetic experiment.

The photoreaction was also monitored by collecting absorption spectra using the spectrophotometer Perkin Elmer Lambda 650. Scanning Electron Microscopy (SEM) analyses were recorded at maximum acceleration voltage of 15 keV at a Hitachi TM3000 Tabletop SEM with a Quantax EDX Detector (Bruker) for Energy Dispersive X-ray (EDX) spectroscopy. Further experiments were conducted using a Zeiss Gemini 500 with an Oxford Ultim Max 100 detector. The samples were prepared on carbon tape without further sputtering.

Thermogravimetric Analyses (TGA) were operated using a NETZSCH STA F3 Jupiter under inert gas atmosphere with a heating rate of 10 K/min (30 °C – 1000 °C).

X-Ray-Diffraction (XRD) patterns were recorded at a Bruker D8 Discover X-Ray Diffractometer with a LYNXEYE and a VANTEC-500 detector with an excitation wavelength of $\lambda_{Cu,K\alpha} = 154$ pm. Depending on the detector, the sample was measured from 7 to 50° (2 θ), for 2 s per step (LYNXEYE), 20 to 50° (2 θ) for 2000 s per step (VANTEC). Data evaluation was carried out using the Bruker DIFFRAC.SUITE EVA software and the Crystallography Open Database (COD).

pH values were determined with a SCHOTT laboratory pH Meter CG 843P at room temperature.

Potentiometric titration experiments were carried out using a TitrandoSys Titrando905 by Metrohm with a 956 Conductivity Module and an 867 pH Module with the titration software tiamoTM. The autotitration setup was equipped with a pH electrode (flat membrane, Metrohm), a Ca-ion-selective electrode (Ca-ISE, Metrohm), a conductivity electrode and an optrode (470 nm). The Ca-ISE was calibrated by titrating calcium chloride solutions to water.

Irradiation by UV/Vis lamp was carried out using a SYLVANIA F8T5/BLB lamp enchased in a Camal case (366 nm).

Irradiations with a LED were done by a Mouser Electronics LuxiGen LZ1 LED Engin. Coodenkey CP3010S DC power supply was used (366 nm, 4.18 V; 0.755 A).

Irradiation for photoreaction quantum yield measurements was performed using a spectrofluorometer by Horiba using Fluoromax-4 at 365 nm (excitation slit 20 nm).

Laser experiments were performed using a frequency-tripled nanosecond Nd:YAG-laser by Continuum. The intensity was adapted for each experiment and is given in the text.

Gel preparation

A 60 % sucrose stock solution in water was prepared. Agarose (20 mg/mL) was dispersed in the sucrose solution and the dispersion was heated in a water bath. After dissolving the solution was directly injected in between two glass slides and was allowed to gelatinize.

4NPP solution preparation

4NPP was dissolved in water regarding the desired concentration (1 mM, 20 mM) and calcium chloride was added. Ratio 4NPP to CaCl₂ 1 eq:1.67 eq. The pH was adjusted between 12 and 13.

The aqueous stock solutions were handled under ambient conditions including CO₂ from the air. For the degassed samples, all stock solutions were degassed prior to mixing for half an hour with nitrogen gas. Additionally, for the so-called degassed precipitate, the irradiation process was executed in a sealed quartz vessel. Nonetheless, when transferring the solutions from the stock solution into the vessel and during the closure, an exposition to a small amount of ambient CO₂-containing air cannot be excluded.

For each characterization of the precipitate, the 1 mM solution was irradiated for 2 h with a UV/Vis lamp and the resulting precipitate was washed with water, ethanol and dichloromethane, as well as dried afterwards. For the kinetic studies as well as the quantum yield, samples were taken after the mentioned time points.

The 20 mM solution was used for the local precipitation process inside the gel matrix.

Local precipitation process

The pre-prepared agarose-sucrose gel was dialyzed with the pre-prepared 20 mM 4NPP solution by putting the gel into the 4NPP solution and letting it soak for 2 hours and repetition of this process with new solution three times. Afterwards, the irradiation with a pulsed laser was carried out according to the image in the main text in scheme 1 A). A total area of 1 cm was irradiated, whereas the slit width of the used grid was 0.5 mm. The irradiation was conducted for 8 minutes. After irradiation, the remaining starting 4NPP solution as well as byproduct were dialyzed out of the gel using water at pH 12-13 by putting the gel into the solution for 2 hours and repetition of this process with new solution three times. The gel was lyophilized.

Photoreaction Quantum Yield

Photoreaction quantum yield was measured by irradiating 4NPP 1 mM solution in NaOH 0.05 M (pH 12-13) and in the presence of CaCl₂ 1.67 mM. Irradiation was performed for 50 minutes in the

spectrofluorometer. Photon flux ($q_{p,in} = 0.95 \times 10^{16}$) was calculated using potassium ferrioxalate as actinometer.^[1, 13] The photoreaction was also monitored by collecting absorption spectra of the diluted solution (1:10) every 10 minutes of irradiation, using the spectrophotometer.

General Procedure of the Titration Experiments

50 mL of the particular aqueous stock solution (1 mM) were adjusted to pH between 12 and 13 via auto titration, using a titration program adding NaOH (0.1 M) dropwise. The calcium titrations were carried out by the addition of a 2 mM CaCl₂ stock solution with an addition rate of 0.01 $\frac{\text{mL}}{\text{min}}$. The pH was kept constant between 12 and 13 by cotitrating NaOH (0.1 M). The titration setup was equipped with a pH electrode, a Ca-ISE electrode, an optrode (470 nm) and a conductivity electrode measuring the pH, the content of calcium, the transmittance, and the conductivity in situ.

Heating Process of the Final Precipitate

The heated precipitate was formed during the thermogravimetric measurement. The precipitate was heated under inert gas atmosphere with a heating rate of 10 K/min (30 °C – 1000 °C).

Chemicals

The chemicals used in this communication were purchased and used without further purification. Details and suppliers are listed in **Table 3**. When the use of water is mentioned, this refers to water purified by a Milli-Q Direct 8 machine from Millipore (18.2 MΩ, 25 °C).

Table 3. Chemicals and solvents used for this paper, including their purities, respectively concentrations and suppliers.

Chemical	Details	Supplier
4-Nitrophenol	> 99.0 %	TCI chemicals
4-Nitrophenylphosphate disodium salt hexahydrate	97+ %	Alfa Aesar (ThermoFisher)
Ammonium dihydrogen phosphate	for analysis	Merck
Calcium chloride solution	1 M	Honeywell
Dichloromethane	> 99.5 % for synthesis	Carl Roth
Ethanol	≥ 99.8 %, p.a. ROTIPURAN®	Carl Roth
Hydrochloric acid solution	0.1 N (Titripur)	Merck
Isopropanol	100 %	VWR
LE Agarose	for gel electrophoresis gel strength (1 %): ≥ 1200 g/cm ²	Biozym Scientific

Methanol	≥ 99.8 % (GC)	Merck
Sodium hydroxide solution	1 N (Titripur)	Merck
Sodium hydroxide solution	0.1 N (Titripur)	Merck
Sucrose	for microbiology	Merck

References

- [1] A. Juris, L. Moggi and M. T. Gandolfi, *Manuale del fotochimico. Tecniche e metodologie*, **2006**, p.
- [2] a) J. C. Elliott, *Structure and Chemistry of the Apatites and Other Calcium Orthophosphates*, Elsevier Science, **1994**, p. 404; b) T. Kaia, K. Gross, L. Plüduma and M. Veiderma, *Journal of Thermal Analysis and Calorimetry* **2011**, 110.
- [3] M. N and S. Murugesan, *International Journal of Nanomedicine* **2015**, 10, 99.
- [4] https://www.chemicalbook.com/SpectrumEN_4264-83-9_13CNMR.htm, (accessed: 24.11.2020).
- [5] http://www.molbase.com/en/hnmr_100-02-7-moldata-32821.html, (accessed: 24.11.2020).
- [6] R. W. McDowell and I. Stewart, *Chemistry and Ecology* **2005**, 21, 211-226.
- [7] L. Tortet, J. R. Gavarrı, G. Nihoul and A. J. Dianoux, *Journal of Solid State Chemistry* **1997**, 132, 6-16.
- [8] M. Hesse, H. Meier and B. Zeeh, *Spektroskopische Methoden in der organischen Chemie*, Georg Thieme Verlag, **2005**, p. 468.
- [9] F. Peters in *Biologische Kristallisation von Calciumphosphaten - Untersuchung und Simulation, Vol. Doktorwürde Universität Hamburg*, Hamburg, **2001**, p. 277.
- [10] H. El Feki, J. Michel Savariault, A. Ben Salah and M. Jemal, *Solid State Sciences* **2000**, 2, 577-586.
- [11] C. B. Baddiel and E. E. Berry, *Spectrochimica Acta* **1966**, 22, 1407-1416.
- [12] H. El Feki, C. Rey and M. Vignoles, *Calcified Tissue International* **1991**, 49, 269-274.
- [13] M. Montalti, A. Credi, L. Prodi and M. T. Gandolfi, **2006**.